Egyptian J. Nucl. Med., Vol. 30, No. 1, June 2025

Original Article, PET/CT.

Optimization of Iterative Image Reconstruction in PET/CT Imaging Procedures: A Patient-Centered Approach.

Moustafa M.[1], Elsayed T.[1], Kany A.[1], EL-Maghraby Sh.[2]

[1]Department of Physics, Faculty of Science, Al-Azhar University, Cairo, Egypt. [2]Nuclear Medicine and Radiation Oncology Department, Cairo University Hospital Faculty of Medicine, Cairo University, Egypt.

ABSTRACT:

Aim: The goal of this study is to optimize image quality metrics including Signal-to-Noise Ratio (SNR), Contrast-to-Noise Ratio (CNR), and Lesion-to-Background Ratio (LBR) while maintaining consistent Standardized Uptake Value ($SUV_{(g/ml)}$) measures using patient and phantom data. The optimized reconstruction parameter were compared with the default reconstruction parameter sets of the General Electric Discovery IQ PET/CT (GE-IQ) and the United Imaging PET/CT (uMI550) scanners. **Results**: Image quality analysis demonstrated wide variations in SUV_{max}, SUV_{mean}, SNR, CNR, and LBR across different reconstruction parameters in both scanners. In GE-IQ scanner, parameter sets utilizing optimized Z-axis weighting, specific iteration and subset, reduced Full Width at Half Maximum (FWHM) consistently outperformed other approaches, including the default parameter set, by delivering higher SUV values and improved image quality. Similarly, in the uMI550 scanner, a parameter set incorporated tighter FWHM, increased subset configurations, and a smoothing filter demonstrated superior image quality and diagnostic accuracy. Overall, the optimized parameter sets on the GE-IQ and uMI550 scanners exhibited a pronounced enhancement in image quality metrics, indicating its superior effectiveness for diagnostic applications, when compared to default parameter sets that recommended by the vendor of each scanner. **Conclusions**: The findings underscore the potential of optimizing reconstruction techniques in PET/CT imaging. Parameter set 39 (Z-axis filter = heavy, iteration = 2, subsets = 12, FWHM = 5.0 mm) in GE-IQ and parameter set 8 (Filter = smoothing1, iteration = 2, subsets = 20, FWHM =3.0 mm) in uMI550 scanners demonstrated superior performance, offering promising avenues for enhancing patient outcomes and advancing medical imaging practices.

Keywords: Image reconstruction, image quality, detection task, PET/CT, SUV

Corresponding author: Sherif El-Maghraby **E-mail:** ry_maghraby@hotmail.com

Submission date: 31/01/2025 **Acceptance date**: **23/04/2025**

INRODUCTION:

Positron emission tomography/computed tomography (PET/CT) has revolutionized medical diagnostics by integrating molecular and anatomical imaging, particularly in oncology and neurology. Image reconstruction is fundamental to this process, converting raw data into clinically interpretable images. Iterative algorithms such as Ordered Subset Expectation Maximization (OSEM) and Maximum Likelihood Expectation Maximization (MLEM) enhance resolution, accuracy, and quantification.[1]. However, factors like noise amplification, suboptimal initial estimates, and computational costs necessitate trade-offs between image quality and quantitative accuracy[2, 3]. Techniques such as Time-of-Flight (TOF) and Point Spread Function (PSF) modeling are employed to optimize metrics like Signal-to-Noise Ratio (SNR) and Contrast-to-Noise Ratio (CNR), and Lesion-to-Background Ratio (LBR), whereas CNR being particularly critical for lesion detectability and diagnostic precision[4]. Advancements in precision medicine drive continuous innovation in PET/CT reconstruction, optimizing algorithms to address tumor heterogeneity and enhance diagnostic accuracy. Ongoing refinements aim to further improve image quality and quantitative precision, reinforcing PET/CT vital role in modern medical diagnostics. [5]. This study investigates the effects of varying reconstruction parameters on image quality and quantitative performance for the GE Discovery IQ (GE-IQ) and United Imaging (uMI550) PET/CT scanners. Specifically, the analysis explores iteration and subset numbers, filter characteristics, and cut-off values compared with each scanner default reconstruction settings. Unlike conventional approaches that rely solely on phantom studies, this work utilized patient data to evaluate image quality metrics. To ensure the validity and reliability of the findings, phantom studies were subsequently employed as a reference standard for ground truth validation. Therefore, the objective was to assess and refine reconstruction parameters for PET/CT imaging across two different scanner models based on performance metrics derived from patient data analysis.

MATERIALS and METHODS:

Patients:

A total of 40 patients were divided into two groups of 20 cases each. The GE-IQ group (mean age: 54±13 years, mean weight: 63±15 kg, 11 females, 9 males) included 38 lesions of varying sizes and locations. The uMI550 group (mean age: 56±13 years, mean weight: 64±18 kg, 9 females, 11 males) had 43 lesions of different sizes and anatomical positions. For each patient, standardized uptake values (SUVs) were calculated for liver and lesion uptake, with SUV_{max} and SUV_{mean} values computed for both liver and lesions. Patients were fasted for 6 hours before commencing the imaging procedure. Extensive exercises were instructed to be avoided, and injection was carried out in relaxing conditions. Data acquisition was performed with GE-IQ and uMI550 after a single intravenous injection of 234.12±51.7 Mega-Becquerel (MBq) and 248.09±45.8 MBq of 18F-FDG respectively. The scan started approximately 62.85±6.23 min and 60.55±7.9 min post-injection in GE-IQ and uMI550 scanners respectively. Data were required with an acquisition time of 3 min/bed-position in all scanners and with 5-6 bed-position on uMI550 scanner whereas 8-10 bed-position on GE-IQ scanner.

Image Acquisition and Reconstruction:

PET/CT scans were acquired using GE-IQ and uMI550 scanners following standard imaging protocols. For the GE-IQ scanner, 42 reconstruction variants were used to reconstruct the raw PET/CT data, incorporating different Z-axis filters (standard, light, heavy), iterations (1–6), subsets (1–12), and cut-off values (5–7.5). These variations were designed to optimize image quality by adjusting the balance between noise reduction and spatial resolution. Similarly, for the uMI550 scanner, 35 reconstruction parameter variants were used, differing in filter function (smoothing or enhance), iterations (1–6), and subsets (10 or 20). The smoothing filter included multiple configurations with varying iterations and subsets. For each scanner, images were reconstructed using both the default parameter and as well as multiple reconstruction with varying parameters. These parameters were selected to cover a range of reconstruction options, including variations in iteration numbers, subset numbers, filtering and smoothing level.

Quantitative Analysis:

Quantitative analysis of PET/CT images was performed using dedicated software. The images were imported into the GE-IQ advanced workstation (GE AW) and the uMI550 advanced workstation (uMI550 AW). SUV_{max} and SUV_{mean} values were measured for liver and lesions in each reconstruction set. Region of interest (ROI) was drawn over the liver to quantify the liver and lesions SUV_{max} and SUV_{mean}. Both measures have been extensively used in routine practice as SNR of liver and lesions well as research objectives in oncologic PET/CT scans. All patients were absent of any abnormal uptake in the liver abnormal or metastatic disease. Statistical comparisons were made between the default reconstruction and alternative parameter sets to assess differences in SUV metrics with threshold 42% [6]. In addition, SNR, CNR, and LBR were calculated in accordance with the equations provided[7-9]:

$$SNR(Liver) = \frac{SUVmean\ (liver)}{SD(liver)}$$

whereas SD is standard deviation.

$$SNR(Lesion) = \frac{SUVmean(lesion)}{SD(lesion)}$$

CNR

$$CNR = \frac{SUVmean\ (lesion) - SUVmean(liver)}{SD\ (liver)}$$

LBR

$$LBR = \frac{SUVmean\ (lesion)}{SUVmean\ (liver)}$$

Phantom Studies:

To evaluate image quality and reconstruction accuracy, a **Jaszczak** ECT phantom was used. The phantom consists of five fillable spheres with volumes of 0.5, 2, 4, 8, and 16 milliliters (mL) and was scanned using sphere to background ratios of 3:1 and 7:1. PET/CT images of the phantom were acquired using both scanners. Reconstruction of phantom images was carried out using the default reconstruction parameter set and selected parameter sets identified through patient data analysis [10, 11].

Phantom Studies:

To evaluate image quality and reconstruction accuracy, a Jaszczak ECT phantom was used. The phantom consists of five fillable spheres with volumes of 0.5, 2, 4, 8, and 16 milliliters (mL) and was scanned using sphere to background ratios of 3:1 and 7:1. PET/CT images of the phantom were acquired using both scanners. Reconstruction of phantom images was carried out using the default reconstruction parameter set and selected parameter sets identified through patient data analysis [10, 11].

Image Analysis:

Maximum and mean recovery coefficients (RC_{max} and RC_{mean}) were calculated for each sphere in the phantom across different reconstruction parameter sets. Additionally, SNR, CNR and LBR were computed to assess image quality and lesion detectability as the previously mentioned equations were also employed.

RESULTS:

SUV_{max} and SUV_{mean}

Patients:

Figure 1 and 2 present the average SUV_{max} and SUV_{mean} for liver and lesion uptake in the GE-IQ and uMI550 scanners, respectively. In GE-IQ, the default reconstruction set yielded a liver SUV_{max} of 2.6±0.4, while the 42 reconstruction sets produced values ranging from 1.7±0.3 to 3.3±0.6. For SUV_{mean}, the default set averaged 1.9±0.4, with a range of 1.4±0.3 to 2.0±0.4 across different sets. In uMI550, the default reconstruction set resulted in a liver SUV_{max} of 3.0±0.4, while the 35 reconstruction sets ranged from 2.7±0.4 to 3.9±0.7. The SUV_{mean} for the default set was 2.51±0.4, with values ranging from 2.50±0.4 to 2.56±0.4 across different reconstruction parameters. For the average of the SUV_{max} and SUV_{mean} of the lesion in GE-IQ scanner, the default reconstruction parameter set showed a lesion SUV_{max} of 8.1±5.6 over 38 different lesions in 20 patients whereas the values of the 42 reconstruction parameter sets ranged from 1.7±1.2 to 10.2±5.7. The average of the SUV_{mean} of lesions, the different reconstruction parameter sets range was from 1.0±0.7 to 6.1±3.3, whereas the default reconstruction set value was 4.8±3.3. In the uMI550 scanner, the default reconstruction protocol yielded a mean SUV_{max} of 11.3±4.6 across 43 lesions, while the 35 reconstruction parameter sets produced values ranging from 9.8±4.6 to 15.0±6.3. For SUV_{mean}, the default reconstruction set resulted in an average of 7.4±2.0, with the 35 parameter sets demonstrating a range from 6.8±2.2 to 8.9±2.3.

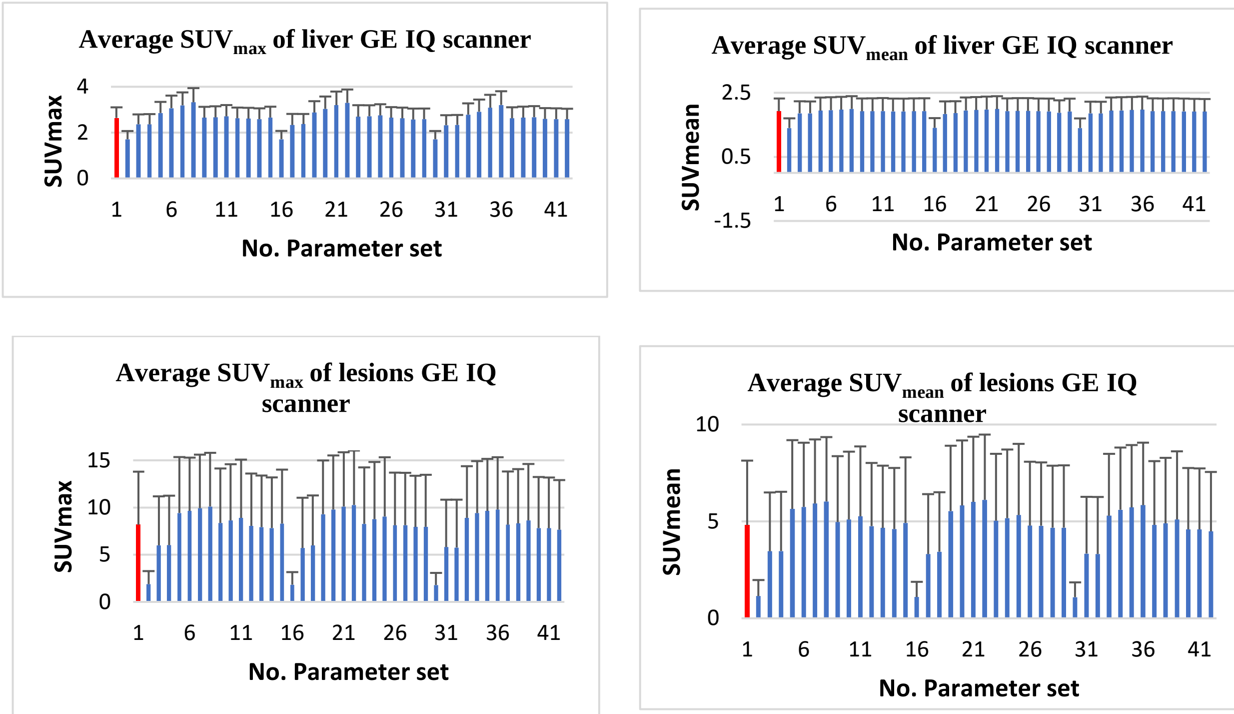

Figure 1. Shows average SUV_{max} and SUV_{mean} of liver and 38 lesion reconstructed using different 42 parameter sets on GE IQ scanner. Colored columns are the recommended parameter set for reconstruction released by scanner vendor.

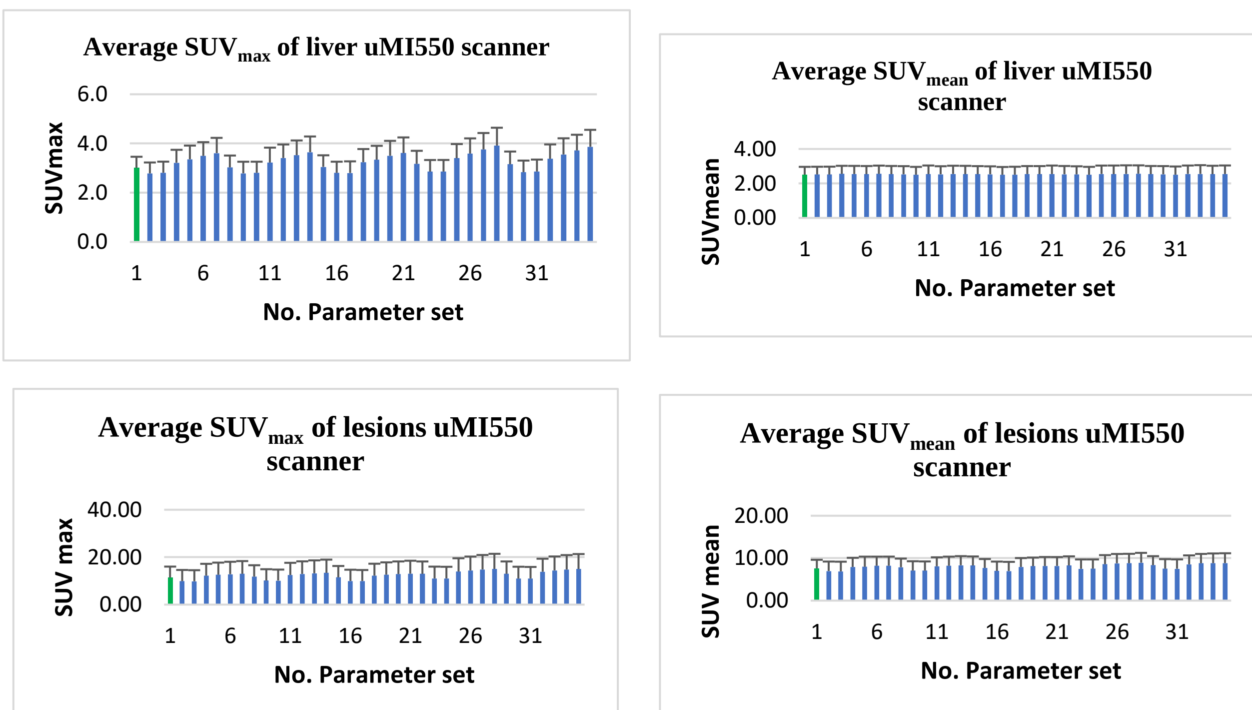

Figure 2. Shows average SUV_{max} and SUV_{mean} of liver and 43 lesion over 35 diffierent reconstruction parameter set on uMI550 scanner. Colored column is the parameter set as recommended by scanner vendor.

Figures 3 and 4 illustrate the reconstruction parameter sets that achieved SNR (liver and lesion), CNR, and LBR values comparable to or exceeding those of the vendor-recommended reconstruction protocol for the GE-IQ and uMI550 scanners. The dashed line represents the reference value of the default reconstruction protocol. Venn diagram is shown in figure 5 representing the distribution of the selected reconstruction parameter sets with common areas of SNR of liver, SNR of lesion, CNR and LBR in GE-IQ and uMI550 scanners. For GE-IQ scanner the selection process revealed about three reconstruction parameter sets that had the highest values of SNR of liver and lesions, CNR, and LBR. Those three parameter sets were the default (Z-axis = standard, iteration = 2, subset = 12, FWHM = 6.4 mm), parameter set 38 (Z-axis = heavy, iteration = 2, subset = 12, FWHM = 5.5 mm) and parameter set 39(Z-axis = heavy, iteration = 2, subset = 12, FWHM = 5.0 mm) respectively. Whereas in uMI550 scanner the process revealed about two reconstruction parameter sets were the vendor (Filter = smoothing3, iteration = 2, subsets = 20, FWHM =3.0 mm) and parameter set 8 (Filter = smoothing1, iteration = 2, subsets = 20, FWHM =3.0 mm).

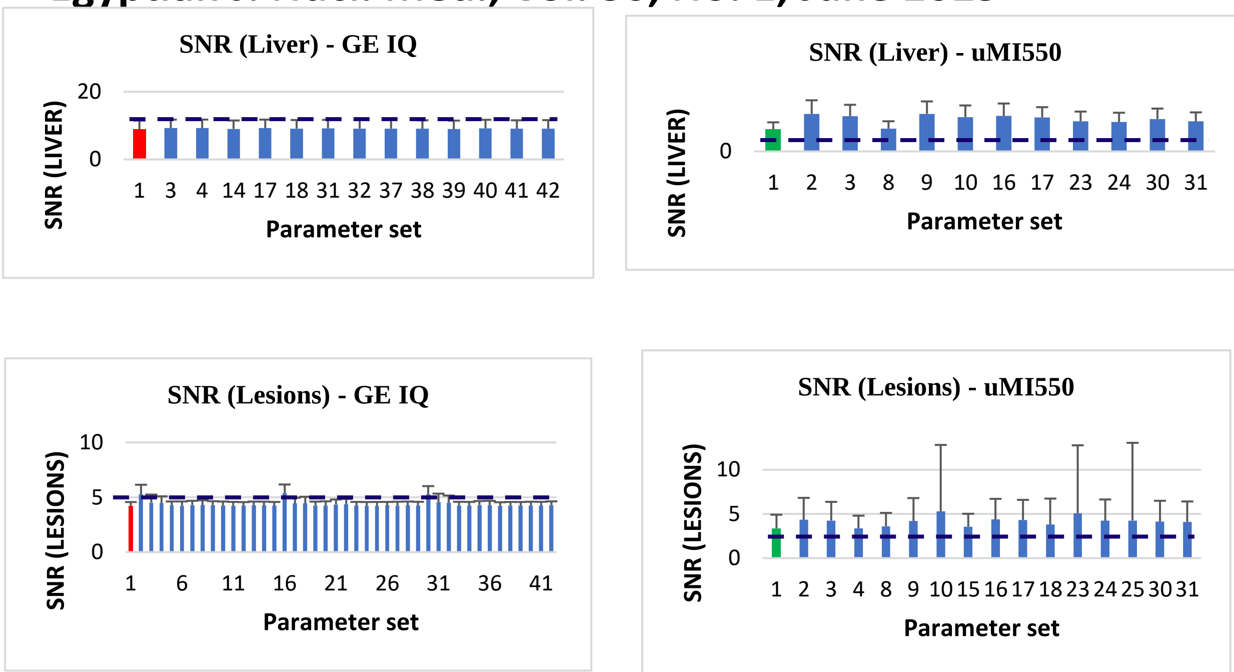

Figure 3. Compilation of those reconstructions that achieved performance better than that of vendor recommendations in terms of liver SNR and lesion SNR in both GE IQ and uMI550 scanners. The dashed line is the limit achieved by vendor recommendations.

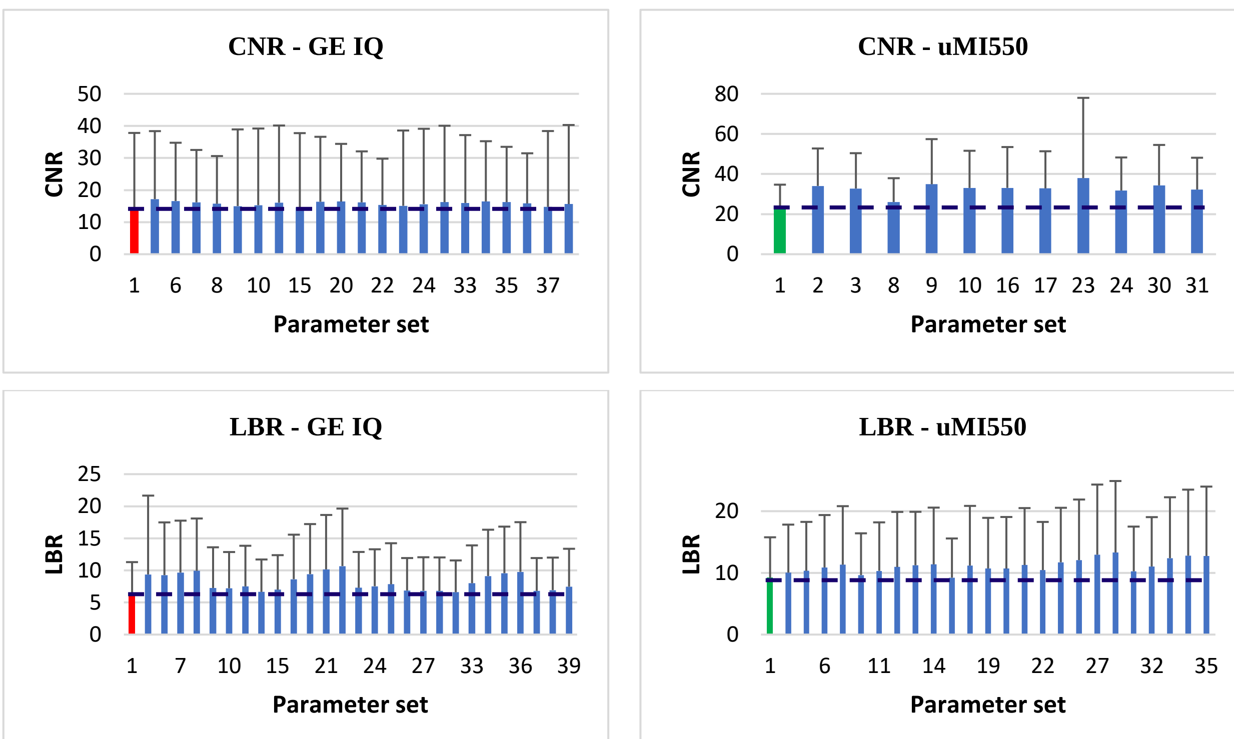

Figure 4. Compilation of those reconstructions that achieved performance better than that of vendor recommendations in terms of CNR and LBR in GE IQ and uMI550 scanners. The dashed line is the limit achieved by vendor recommendations.

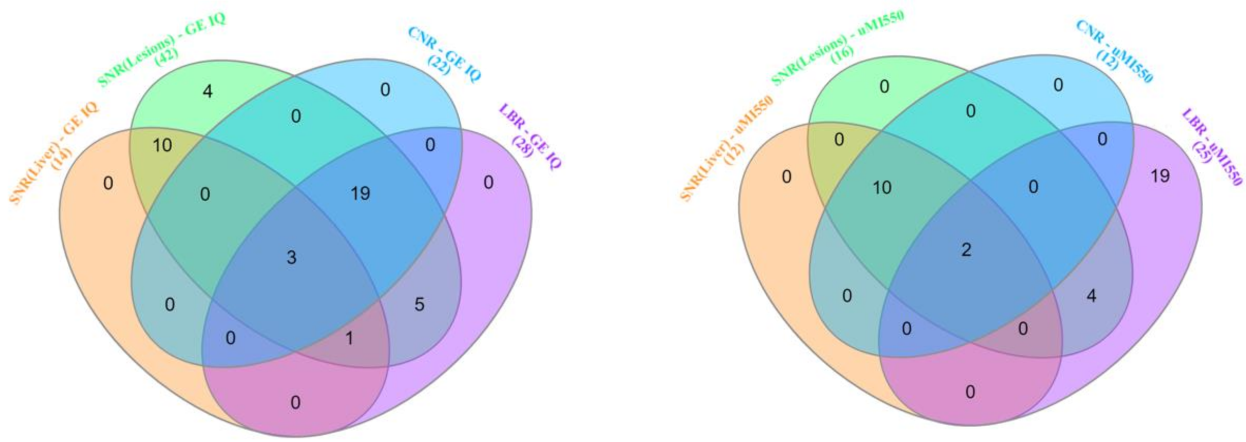

Figure 5. Venn diagrams show common areas of parameter sets with highest average values of SNR (Liver), SNR (Lesions), CNR and LBR on GE IQ scanner and uMI550 scanner.

Phantom:

Jaszczak ECT phantom with five fillable spheres with their standard volumes 0.5 ml , 2ml , 4ml, 8ml and 16 ml were shown in figure 6 with two concentrations 3:1 and 7:1 scanned on GE-IQ and uMI550 scanners of the selected reconstruction parameter sets were revelated. Visual comparisons, as shown in figure 7, underscore these improvements with better contrast and detail resolution compared to default parameter sets.

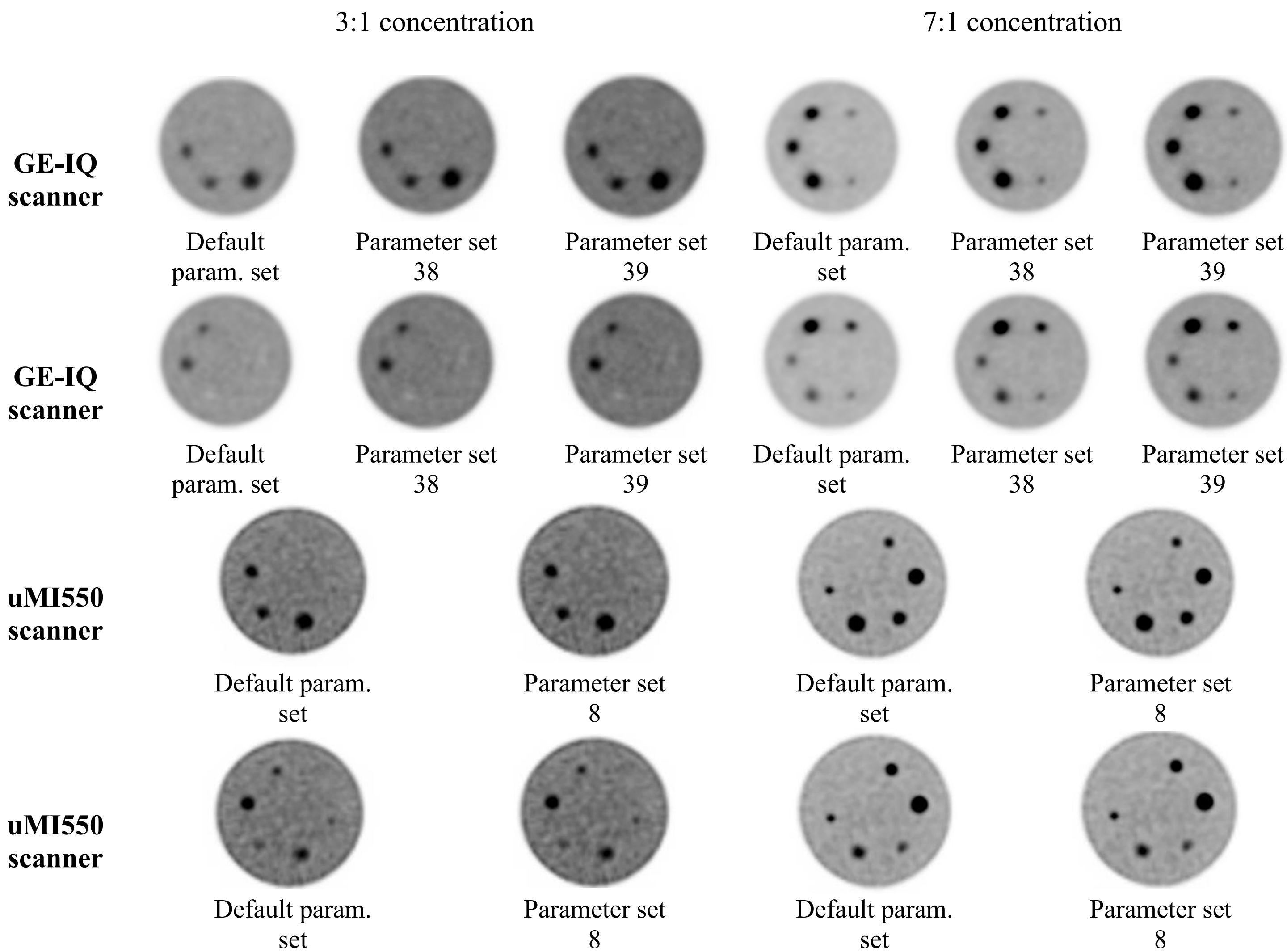

Figure 6. Jaszczak ECT phantom images of concentration 3:1 and concentration 7:1 (Default parameter set, parameter set 38, and parameter set 39) on GE IQ scanner, and (Default parameter set, parameter set 8) on uMI550 scanner.

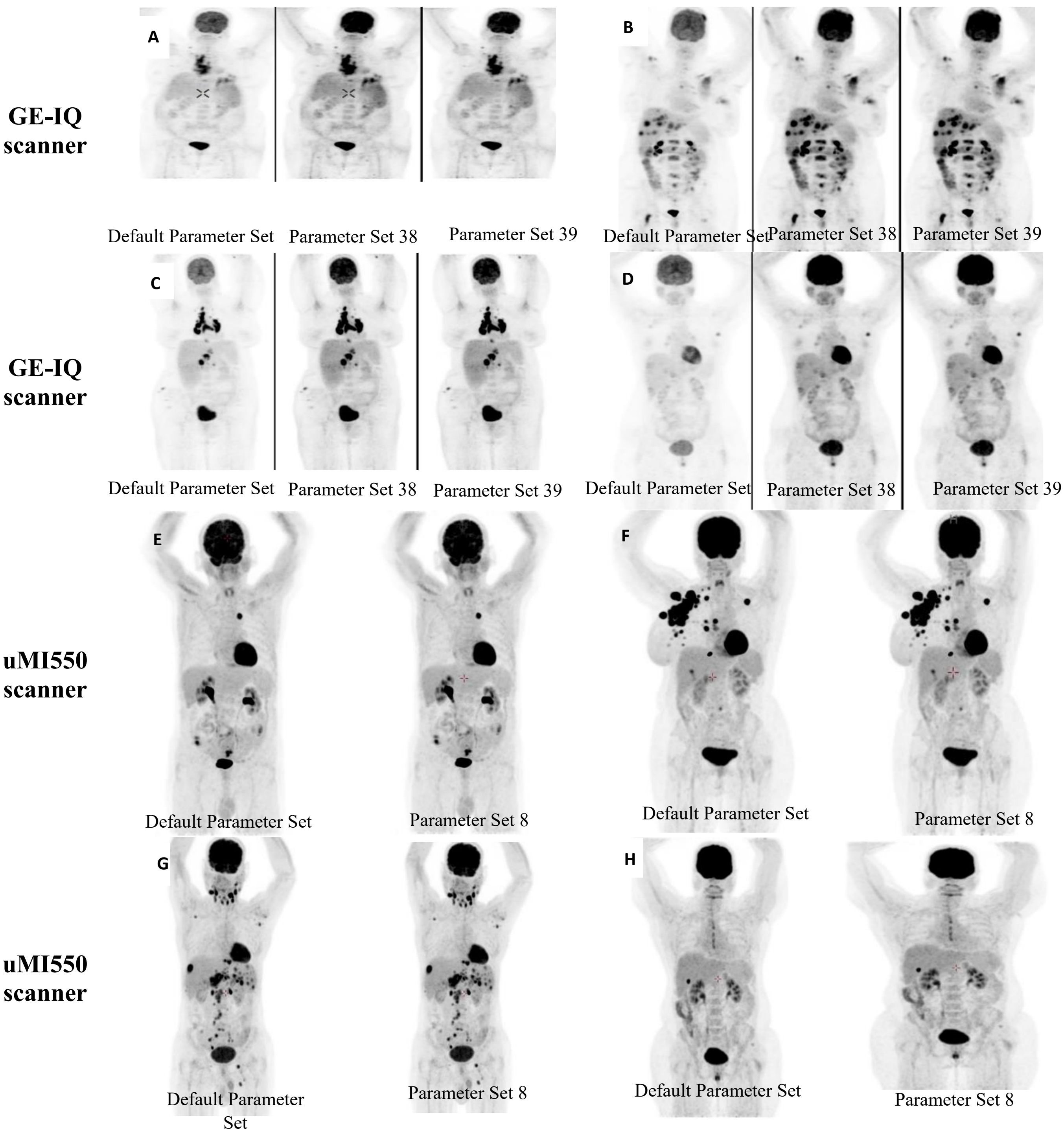

Figure 7. Clinical presentation of the optimized reconstruction parameter sets versus the default sets using GE-IQ (top panel) and uMI550 (lower panel). Examples provided are for A) lung, B) breast, C) lung, D) lymphoma, E) lung, F) breast, G) lymphoma, and H) l lymphoma cancers. Optimization in GE is represented by paramter set 38 and paramter set 39 whereas in uMI550 is represented by parameter set 8.

DISCUSSION:

PET/CT has emerged as a powerful tool in the diagnosis and management of various diseases, especially cancer. The reconstruction of PET/CT images is vital for ensuring accuracy and quality of information obtained. Traditional methods like filtered back projection have limitations in noise reduction and spatial resolution. In recent years, iterative reconstruction techniques have shown promise in overcoming these challenges and improving the overall performance of PET/CT imaging [12]. Selection and optimization of image reconstruction in PET/CT imaging remains challenging due to several factors that interfere with and impact image quality and quantitative accuracy. Clinical images often have different structures and regions of variable metabolic uptake. Selecting parameters that meet the requirements for various clinical lesions across different patients is challenging. This complexity arises from variations in dose levels, lesion characteristics, and biodistribution among patients [13, 14]. This work attempted to investigate the most appropriate reconstruction parameter sets centered on data derived from patient information and image analysis. The procedure followed is different from many previous reports that started with phantom studies to continue afterward on clinical data. The approach here was to examine the different reconstruction parameter sets available in two different commercial scanners and filter out those parameter sets that could provide elevated estimate of image quality metrics including SNR, CNR and LBR while keeping consistent measures of SUV [15, 16]. This study aimed in principle to identify optimal reconstruction sets by analyzing clinical data from 40 cases, divided equally between GE-IQ and uMI550 imaging scanners. The focus was on determining reconstruction sets that enhance key image quality and quantitative accuracy of PET/CT images. Parameter set 38 and 39 were identified as superior to the default set for GE-IQ, with parameter set 39 consistently demonstrating higher performance. It showed significant improvements in CNR and LBR, enhancing lesion visibility and diagnostic clarity. While parameter set 38 exhibited better SNR for lesions, parameter set 39 outperformed it in most metrics, making it the preferred choice for clinical use. For the uMI550 scanner, parameter set 8 emerged as the most effective, outperforming the default parameter set across all evaluated metrics. It demonstrated significant enhancements in SNR for both liver and lesions, as well as superior CNR and LBR, leading to better lesion distinguishability and background noise reduction. These results indicate that parameter set 8 holds strong clinical potential for improving image quality and diagnostic accuracy in uMI550 scanner. Validation using phantom imaging further supported these findings. Recovery coefficient of SUV_{mean} was calculated for Jaszczak ECT phantom spheres with concentration ratios (3:1 and 7:1) using the GE-IQ and uMI550 scanners. The recovery coefficient reflects scanner ability to accurately quantify activity in regions of interest, which is particularly challenging for smaller spheres due to partial volume effects. Optimized reconstruction parameters significantly improved recovery coefficients, especially for smaller spheres, by incorporating refined reconstruction settings such as tighter smoothing kernels (narrower FWHM) and optimized iteration and subset configurations, enhancing spatial resolution. These adjustments reduced spill out effects, improving quantitative accuracy. Among the tested reconstruction parameter on the GE-IQ scanner, parameter set 39 consistently outperformed both the default and parameter set 38. Its superior results stem from a balance between enhanced spatial resolution and effective noise suppression. Narrower FWHM improved lesion boundary delineation, while optimized iteration and subset values minimized noise amplification. The observed increases in CNR and LBR further highlight improved lesion contrast against the background, crucial for accurate lesion detection and characterization. For the uMI550 scanner, demonstrating the impact of optimized reconstruction parameters on image quality, parameter set 8 exhibited marked improvements in these metrics compared to the default method, particularly for smaller sphere volumes. This enhancement is attributed to the incorporation of a smoothing filter (smoothing1) and tighter FWHM settings, which effectively reduce noise while maintaining spatial resolution. The optimized parameters ensure better contrast and lesion detectability, particularly in challenging scenarios involving small or low-contrast lesions. The superior performance of parameter set 8 highlights its ability to address the trade-offs between noise suppression and spatial resolution, resulting in enhanced diagnostic capability. The observed improvements in recovery coefficients, SNR, CNR, and LBR across both scanners result from optimized reconstruction parameters that balance spatial resolution and noise reduction. Narrower smoothing kernels minimize blurring and enhance detail recovery, while optimized iteration and subset configurations improve image convergence without excessive noise. These refinements enhance the resolution of small structures and improve lesion-background distinction. Performance differences between the GE-IQ and uMI550 scanners highlight variations in hardware, reconstruction algorithms, and default settings, emphasizing the need for scanner-specific optimization. Parameter set 39 consistently outperformed others on GE-IQ, demonstrating superior SUV_{max} and SUV_{mean} values across sphere volumes and concentration ratios. Similarly, parameter set 8 for uMI550 significantly improved SUV metrics, particularly for smaller spheres. These findings underscore the clinical value of optimized reconstruction settings in enhancing PET/CT imaging quality by reducing noise, improving resolution, and ensuring consistent metabolic signal differentiation.

Limitation of the study:

- The study did not account for variations in patient physiology, such as metabolic differences and different injected radiotracer doses, which could influence SUV measurements, image contrast, and overall image quality.
- Phantom validation was conducted under controlled conditions, which may not fully replicate real clinical scenarios with patient-specific complexities, including variations in lesion types, sizes, and locations.
- The study focused on static PET/CT imaging and did not explore potential differences in dynamic imaging protocols, which could impact reconstruction performance and diagnostic accuracy.

Future plan:

Optimizing PET image reconstruction for a given scanning system maximizes its imaging capabilities, enhancing image interpretation and diagnostic accuracy. Artificial intelligence (AI) plays a crucial role in image acquisition, processing, and analysis but relies heavily on high-quality input data. Thus, utilizing the best imaging data from a given scanner is essential for developing robust AI models. While this study does not directly focus on AI, its findings serve as foundational prerequisites for AI-driven improvements in lesion detection and image quality. Future work will integrate these optimized reconstruction methods into AI models, with the choice of deep learning architectures (e.g., convolutional or recurrent neural networks) tailored to specific tasks and data characteristics. Our research group aims to incorporate the proposed pipeline into advanced AI models to refine imaging outcomes and enhance quality measures, ensuring more reliable and precise PET image analysis.

CONCLUSIONS:

Based on the comprehensive analyses of the GE-IQ and uMI550 reconstruction parameter, significant and improved measures of image and quantitative accuracy could be attained. Parameter set 39 on GE-IQ and parameter set 8 on uMI550 showed superior performance in improving SUV values, SNR, CNR, and LBR, enhancing lesion visibility and diagnostic accuracy compared to their default parameter sets. These improvements are attributed to optimized smoothing parameters, which enhance spatial resolution and reduce noise, making lesions more distinguishable.

REFERENCES:

1. **Kluetz, P. G., and Meltzer, C. C.** Combined PET/CT imaging in oncology: impact on patient management. Clin.l Posi. Imag. 3(6): p. 223-30, **2000**.
2. **Herman, G. T., and Odhner, D.,** Performance evaluation of an iterative image reconstruction algorithm for positron emission tomography. IEEE Trans. Med. Imaging. 10(3): p. 336-46, **1991**.
3. **Su, X., and Geng, J.,** Influence of reconstruction techniques on PET/CT image quality and quantitative accuracy: a phantom study. Radiation Detection Technology and Methods. 8(2): p. 1171-86, **2024**.
4. **Shekari, M., and Ghafarian, P.,** Quantification of the impact of TOF and PSF on PET images using the noise-matching concept: clinical and phantom study. Nucl. Sci. Tech. 28: p. 1-8, **2017**.
5. **Ha, P. K., Hdeib, A., et al.,** The role of positron emission tomography and computed tomography fusion in the management of early-stage and advanced-stage primary head and neck squamous cell carcinoma. Arch. Otolaryngol. Head Neck Surg. 132(1): p. 12-6, **2006**.
6. **Jaskowiak, C. J., and Bianco, J. A.** Influence of reconstruction iterations on 18F-FDG PET/CT standardized uptake values. J. Nucl. Med. 46(3): p. 424-8, **2005**.
7. **Huang, K., and Feng, Y.,** Impact of time of flight and point spread function on quantitative parameters of lung lesions in 18 F-FDG PET/CT. BMC Med. Imaging. 21: p. 1-9, **2021**.
8. **Øen, S. K., Aasheim, L. B., et al.,** Image quality and detectability in Siemens Biograph PET/MRI and PET/CT systems—a phantom study. EJNMMI physics. 6: p. 1-16, **2019**.
9. **Cherry, S., and Sorenson, J.,** Chapter 15-Image Quality in Nuclear Medicine. Physics in nuclear medicine. 4th ed. Philadelphia: WB Saunders. 233-51, **2012**.
10. Silosky, M., Chin, B., Modelling small lesion CNR in clinically relevant phantom studies., Soc Nuclear Med, **2022**.
11. **Sadeghi, F., and Sheikhzadeh, P.,** The effects of various penalty parameter values in Q. Clear algorithm for rectal cancer detection on 18F-FDG images using a BGO-based PET/CT scanner: a phantom and clinical study. EJNMMI physics. 10(1): p. 63, **2023**.
12. **Sattler, B., and Lee, J. A.,** PET/CT (and CT) instrumentation, image reconstruction and data transfer for radiotherapy planning. Radiat. Oncol. J. 96(3): p. 288-97, **2010**.
13. **Hsiao, T., and Khurd, P.,** An overview of fast convergent ordered-subsets reconstruction

methods for emission tomography based on the incremental EM algorithm. Nuclear Instruments and Methods in Physics Research Section A: Accelerators, Spectrometers, Detectors and Associated Equipment. 569(2): p. 429-33, **2006**.

14. **Søndergaard, H. M., Madsen, M. M., et al.,** Evaluation of iterative reconstruction (OSEM) versus filtered back-projection for the assessment of myocardial glucose uptake and myocardial perfusion using dynamic PET. Eur. J. Nucl. Med. Mol. Imag. 34: p. 320-9, **2007**.

15. **Alzimami, K. S., and Sassi, S. A.,** A comparison between 3D OSEM and FBP image reconstruction algorithms in SPECT. Adv. Electr. Comp. Eng.: p. 195-206, **2009**.

16. **Du, J., and Ariño-Estrada, G.,** Performance comparison of dual-ended readout depth-encoding PET detectors based on BGO and LYSO crystals. Phys. Med. Biol. 65(23): p. 235030, **2020**.